Biogeosciences Discuss., 11, 16599–16643, 2014
www.biogeosciences-discuss.net/11/16599/2014/
doi:10.5194/bgd-11-16599-2014

Biogeosciences
Discussions
Open Access

Observation-based modelling of permafrost carbon fluxes with accounting for deep carbon deposits and thermokarst activity

T. Schneider von Deimling[1,2], G. Grosse[2], J. Strauss[2], L. Schirrmeister[2], A. Morgenstern[2], S. Schaphoff[1], M. Meinshausen[3], and J. Boike[2]

[1]Potsdam Institute for Climate Impact Research, Potsdam, Germany
[2]Alfred Wegener Institute Helmholtz Centre for Polar and Marine Research, Periglacial Research Unit, Potsdam, Germany
[3]School of Earth Sciences, The University of Melbourne, Victoria, Australia

Received: 25 September 2014 – Accepted: 23 October 2014 – Published: 3 December 2014

Correspondence to: T. Schneider von Deimling (schneider@pik-potsdam.de)

Published by Copernicus Publications on behalf of the European Geosciences Union.

Abstract

High-latitude soils store vast amounts of perennially frozen and therefore inert organic matter. With rising global temperatures and consequent permafrost degradation, a part of this carbon store will become available for microbial decay and eventual release to the atmosphere. We have developed a simplified, two-dimensional multi-pool model to estimate the strength and timing of future carbon dioxide (CO_2) and methane (CH_4) fluxes from newly thawed permafrost carbon (i.e. carbon thawed when temperatures rise above pre-industrial levels). We have especially simulated carbon release from deep deposits in Yedoma regions by describing abrupt thaw under thermokarst lakes. The computational efficiency of our model allowed us to run large, multi-centennial ensembles under various scenarios of future warming to express uncertainty inherent to simulations of the permafrost-carbon feedback.

Under moderate warming of the representative concentration pathway (RCP) 2.6 scenario, cumulated CO_2 fluxes from newly thawed permafrost carbon amount to 20 to 58 petagrammes of carbon (Pg-C) (68 % range) by the year 2100 and reach 40 to 98 Pg-C in 2300. The much larger permafrost degradation under strong warming (RCP8.5) results in cumulated CO_2 release of 42–141 and 157–313 Pg-C (68 % ranges) in the years 2100 and 2300, respectively. Our estimates do only consider fluxes from newly thawed permafrost but not from soils already part of the seasonally thawed active layer under preindustrial climate. Our simulated methane fluxes contribute a few percent to total permafrost carbon release yet they can cause up to 40 % of total permafrost-affected radiative forcing in the 21st century (upper 68 % range). We infer largest methane emission rates of about 50 Tg-CH_4 year^{-1} around the mid of the 21st century when simulated thermokarst lake extent is at its maximum and when abrupt thaw under thermokarst lakes is accounted for. CH_4 release from newly thawed carbon in wetland-affected deposits is only discernible in the 22nd and 23rd century because of the absence of abrupt thaw processes. We further show that release from organic matter stored in deep deposits of Yedoma regions does crucially affect our

BGD

11, 16599–16643, 2014

Observation-based modelling of permafrost carbon fluxes

T. Schneider von Deimling et al.

simulated circumpolar methane fluxes. The additional warming through the release from newly thawed permafrost carbon proved only slightly dependent on the pathway of anthropogenic emission and amounts about 0.03–0.14 °C (68 % ranges) by end of the century. The warming increased further in the 22nd and 23rd century and was most pronounced under the RCP6.0 scenario with adding 0.16–0.39 °C (68 % range) to simulated global mean surface air temperatures in the year 2300.

1 Introduction

Soils in high northern latitudes represent one of the largest reservoirs of organic carbon in the terrestrial biosphere, holding an estimated 900–1700 petagramms (Pg) of organic carbon (Hugelius et al., 2014). While portions of this carbon pool are already affected by seasonal thaw in the active layer, substantial amounts are locked in perennially frozen deposits at depths currently exceeding the seasonal thaw depth. Zimov et al. (2006) have estimated that an amount of 450 Pg-C is stored in deep Siberian organic-rich frozen loess and have speculated that this carbon store could significantly contribute to global carbon fluxes when thawed. A more recent study based on updated observations estimates a total of 211 (58–371) Pg-C being stored in ice- and carbon-rich deep deposits in Siberia and Alaska (Strauss et al., 2013). As long as frozen in the ground, permafrost organic matter is not part of the active carbon cycle and can be considered mainly inert. With sustained warming and subsequent degradation of deeper permafrost deposits, a part of this carbon pool will become seasonally thawed. Consequently, it will become prone to microbial decomposition and mineralization. By ultimately increasing the atmospheric concentration of the greenhouse gases CO_2 and CH_4, the carbon release from thawing permafrost regions is considered a potentially large positive feedback in the climate-carbon system (Schaefer et al., 2014). Given the long millennial timescale processes leading to the build-up of old carbon in permafrost soils, future rapid releases from these deposits are irreversible on a human timescale.

BGD
11, 16599–16643, 2014

However, the magnitude and timing of carbon fluxes as a consequence of permafrost degradation are highly uncertain. This is mainly due to incomplete observational knowledge of the amount of organic matter stored in permafrost deposits, of its quality and decomposability, as well as due to the challenge of modelling the full chain of processes from permafrost thaw to carbon release. Furthermore, conceptual and numerical permafrost landscape models also require suitable upscaling methods ranging from local to global scales, based on field-based knowledge of the surface characteristics, key processes and data collection of key parameters (Boike et al., 2012). The vulnerability of permafrost carbon and its fate when thawed will be strongly determined by various environmental controls (Grosse et al., 2011) such as soil type and soil moisture, which both affect soil thermal conductivity and therefore determine the timescale of heat penetration into the ground. Additionally, surface conditions such as organic-rich soil surface layers, vegetation cover and snow exert strong controls on subsurface temperatures by insulating the ground from surface air temperatures (Koven et al., 2013a). Mineral permafrost soils are typically more vulnerable to degradation than carbon-rich organic soils: the often higher ice-content of the latter requires a larger energy input for phase transition and the usually anaerobic environments in organic soils slow down carbon mineralization. Therefore, for capturing site-specific pathways of carbon release from permafrost degradation, it is important to consider the differing soil environments under which the organic matter will be thawed. Of key importance is the impact of hydrological conditions which determine whether mineralized carbon will be emitted as CO_2 or CH_4 (Olefeldt et al., 2013). Future changes in hydrological conditions in permafrost regions will therefore crucially affect the high latitude carbon balance. Especially regions of ice-rich late Pleistocene deposits (Yedoma) are considered to become potential hot spots for intensive thermokarst lake formation with consequent increases in the fraction of permafrost-affected sediments under anaerobic environments (Walter et al., 2007a). Apart from affecting hydrological conditions, thermokarst lakes also exert a strong warming of sub-lake sediments and thus enhance abrupt permafrost degradation.

BGD
11, 16599–16643, 2014

If thermokarst lake depths exceed the maximum thickness of winter lake ice, these lakes retain liquid water year-round and provide a strong warming and thawing of the underlying sediments (Arp et al., 2012). As a consequence, mean annual temperatures of thermokarst lake bottom sediments can be up to 10 °C warmer than mean annual air temperatures (Jorgenson et al., 2010).

So far, permafrost carbon dynamics are not included standard climate model projections, possibly due to only recent recognition of the large vulnerable permafrost carbon pool and given the complexity of processes involved. The complexity arises not only from the need to simulate physical changes in soil thermal conditions and phase transitions of water as a consequence of various environmental controls (e.g. interactions among topography, water, soil, vegetation and snow, Jorgenson et al., 2010). It also arises from the challenge of describing the full chain of bio-geochemical processes for eventual carbon decomposition in the soils and release to the atmosphere. Therefore, various aspects of permafrost physics and biogeochemistry are only being implemented into current global climate models (formulated e.g. in Lawrence and Slater, 2008; Koven et al., 2009, 2013b; Lawrence et al., 2011; Dankers et al., 2011; Schaphoff et al., 2013; Ekici et al., 2014). First modelling results suggest a very large range in predicted soil carbon losses from permafrost regions under scenarios of unmitigated climate change (about 20 to 500 Pg-C by 2100, see Schaefer et al. (2014) for an overview). This large range demonstrates the current uncertainty inherent to predictions of the timing and strength of the permafrost carbon feedback.

Yet, these studies are based on models which still miss important mechanisms to capture the full complexity of the permafrost carbon feedback. Grosse et al. (2011) and van Huissteden and Dolman (2012) underline that none of the current permafrost models consider the spatially inhomogeneous and potentially much more rapid degradation of ice-rich permafrost and lake formation. This omission of abrupt thaw processes may result in underestimating an important part of anaerobic soil carbon decomposition. Studies have also underlined the importance of considering small scales: not only large Arctic lakes, but also the smaller Arctic thaw ponds, are

BGD
11, 16599–16643, 2014

biological hotspots for the emission of CO_2 and CH_4 (Abnizova et al., 2012; Laurion, 2010). A recent expert assessment has emphasized the importance of abrupt thaw processes and so far unaccounted carbon stored in deep deposits below three meters (Schuur et al., 2013). Evidence for rapid and abrupt thaw on decadal scale, is already widespread (Jorgenson et al., 2006; Sannel and Kuhry, 2011; Kokelj et al., 2013; Raynolds et al., 2014), is likely to increase with future warming, and thus needs to be considered in order to make realistic projections of carbon dynamics in permafrost regions.

Our study aims to estimate the range of potential carbon fluxes from thawing permafrost by accounting for abrupt thaw processes which can accelerate the degradation of frozen ground beyond what is inferred by standard modelling approaches that consider gradual thaw. By explicitly modelling carbon releases from deep carbon stores below three meters, we contribute to a more complete quantification of the permafrost-carbon feedback. By allocating permafrost organic matter into pools of differing environmental controls, we describe different pathways of carbon release and we especially account for carbon released as methane which is mostly neglected in current modelling approaches. Similarly, permafrost carbon release from deep deposits is mostly not accounted for, although first modelling studies have considered the contribution of permafrost carbon in Yedoma regions (Koven et al., 2011; Schaphoff et al., 2013). Yet in these studies the deep deposits have not contributed significantly to simulated carbon release because the models did not describe abrupt thaw processes. Khvorostyanov et al. (2008) have inferred a large contribution from Yedoma carbon deposits after the year 2300 when assuming that microbial heat strongly speeds-up permafrost degradation. To the best of our knowledge, our modelling approach is the first to globally quantify the permafrost-carbon feedback for the coming centuries under considering carbon release from deep deposits and accounting for abrupt thaw processes.

BGD
11, 16599–16643, 2014

2 Multi-pool permafrost model

Building on previous work (Schneider von Deimling et al., 2012), we have developed a simplified large-scale two-dimensional model with parameters tuned to match observed permafrost carbon characteristics. The model calculates permafrost degradation and eventual CO_2 and CH_4 release under differing environmental conditions. The newly developed model is shortly described in the following sections while more details are given in the Supplement.

The model accounts for several processes which are key to the permafrost carbon feedback:

1. Depending on soil-physical factors, hydrologic conditions, and organic matter quality, permafrost carbon inventories were sub-divided into a total of 24 pools.

2. Permafrost thaw was calculated for various scenarios of global warming to determine the amount of carbon vulnerable to eventual release. Anaerobic soil fractions were calculated to determine the amount of organic matter stored in wetland- and thermokarst-affected sediments.

3. Permafrost carbon release as either CO_2 or CH_4 was calculated based on typical rates for aerobic and anaerobic carbon release.

4. By using a simplified climate-carbon model, we have determined the additional increase in global mean temperature through the permafrost carbon feedback.

The computational efficiency of our model allows us to explore the range of simulated permafrost carbon feedbacks by running large ensembles. Our proceeding expresses the uncertainty inherent to current knowledge of permafrost carbon release. Our framework allows identifying key model parameters and processes and thus enables us to assess the importance of these factors for shaping the strength and timing of the permafrost carbon feedback.

BGD
11, 16599–16643, 2014

2.1 Model structure

The magnitude and timing of carbon release from thawing permafrost soils will be strongly determined by soil-physical factors such as soil composition and organic matter decomposability, hydrologic state, and surface conditions. To account for these factors, we have developed a simplified but observationally constrained and computationally efficient two-dimensional model which allocates permafrost soil organic matter into various carbon pools. These pools describe carbon amount and quality, soil environments, and hydrological conditions (Fig. 1). To account for deposit-specific permafrost carbon vulnerability, we divide our carbon inventory into two near-surface pools (mineral and organic, 0 to 3 m) and into two deep-ranging pools (Yedoma and refrozen thermokarst (including taberal sediments), 0 to 15 m, see next section and Table 1). By taberal deposits we understand permafrost sediments that underwent thawing in a talik (a layer of year-round unfrozen ground in permafrost areas, such as under a deep lake), resulting in diagenetic alteration of sediment structures (loss of cryostructure, sediment compaction) and biogeochemical characteristics (depletion of organic carbon). In addition, taberal deposits may be subject to refreezing (e.g., after lake drainage) (Grosse et al., 2007).

We describe differing hydrological controls by further subdividing each carbon pool into one aerobic fraction and two anaerobic fractions. Hereby we account for anaerobic conditions provided in wetland soils and by water-saturated sediments under thermokarst lakes. In the following we define wetland soils from a purely hydrological viewpoint, i.e. by assuming that these soils are water-saturated and not affected by thermokarst. We further assume that anaerobic soil fractions are not stationary but will increase or decrease with climate change. Therefore, we re-calculate the wetland and thermokarst fraction for each time step (see the Supplement for model details). We assume a linear increase in wetland extent with global warming with mean maximum increases up to 30 % above pre-industrial wetland extent (see Table 1). To capture changes in future thermokarst lake coverage, we have developed a conceptual model by making the simplifying assumption that future increases in high latitude surface air temperatures are the main driver for thermokarst formation. We hereby assume that future warming results in a gradual increase of thermokarst lake areas (Smith et al., 2005; Plug and West, 2009; Walter et al., 2007b) until a maximum extent is reached (see Table 1). With further warming our model describes a decrease in thermokarst lake extent as we assume that lake drainage is becoming a key factor which strongly limits thermokarst lake area (van Huissteden et al., 2011; Smith et al., 2005; Jones et al., 2011; Morgenstern et al., 2011; see also Fig. S1).

As the quality of organic matter is a further key determinant for the timescale of carbon release (Strauss et al., 2014) we subdivide the carbon of each individual pool into a fast and a slowly decomposing fraction, with annual or respectively decadal timescales (Table 1). We do not describe permafrost organic matter of low quality (passive pool) which decays on a multi-centennial to millennial timescale. The partitioning of permafrost organic matter results in a total of 24 separate carbon pools which all contribute individually to simulated carbon fluxes (Fig. 1).

All pools and processes are stratified along latitudinal bands that provide a simplified gradient of climate and permafrost types. To describe the climate control exerted by surface–air and ground temperatures in each latitude band, we assume that large-scale climate effects can be described by a general north–south temperature gradient. We acknowledge that longitudinal patterns can also be pronounced, but with a focus on large-scale regional rather than local changes we expect that the dominant climate control can be described by a profile of coldest permafrost temperatures at the northern limit and warmest temperatures at the southern limit (Romanovsky et al., 2010; Beer et al., 2013). Our model also resolves vertical information to account for varying carbon density with depth and to track active layer changes. We chose a model resolution of 20 latitudinal bands (which range from 45 to 85° N with a 2° gridding) and of 27 vertical soil layers (corresponding to layer thicknesses of 25 cm for the upper four meters, and of 1 m for the depth range 4 to 15 m).

BGD
11, 16599–16643, 2014

2.2 Model initialization

The flexibility of our model allows us to tune model parameters to observed data, e.g. to permafrost carbon inventories, carbon qualities, or active layer depths. This approach assures that our simulations do not suffer from an initial bias in the amount of modelled permafrost carbon. This is contrary to model studies, which fully simulate soil thermal conditions with potentially large biases in initial permafrost extent (Slater and Lawrence, 2013). Such biases result in a large spread in simulated initial permafrost carbon stores (Mishra et al., 2013; Gouttevin et al., 2012). Based on updated Arctic soil carbon data (Hugelius et al., 2013, 2014; Strauss et al., 2013; Walter Anthony et al., 2014) we allocate permafrost carbon pools (latitudinally and vertically resolved) in different regions: two deep-ranging pools (0 to 15 m) in regions with Yedoma (80 Pg-C) and refrozen thermokarst deposits (240 Pg-C), and two near-surface pools (0 to 3 m) in remaining regions with mineral soils (540 Pg-C) and organic soils (120 Pg-C), see the Supplement and Table 1. We then initialize each latitude band with a mean annual ground temperature between −0.5 and −10 °C based on summer air temperature climatology data from the Berkeley Earth dataset (http://berkeleyearth.org/data see the Supplement). The above temperature range is consistent with observed ground temperatures of continuous and discontinuous permafrost in the Northern Hemisphere (Romanovsky et al., 2010). We do not consider permafrost temperatures below −10 °C (observed in the Canadian Archipelago and Northern Russia) which we consider in the outer tail of permafrost temperature distributions.

By assuming that the equilibrium active layer depth is determined by mean annual ground temperature and by the seasonal cycle of soil temperatures (see Koven et al., 2013a), we calculate typical minimum seasonal thaw depths of about 0.3 m (northernmost permafrost regions) and maximum seasonal thaw of about 2.5 to 3 m (southernmost regions) for present-day climate conditions (see the Supplement). Although topography, soil type, as well as organic layer, vegetation cover, and snow cover variability can lead to spatially very heterogeneous patterns of active layer

BGD
11, 16599–16643, 2014

thicknesses, our scheme describes a latitudinal tendency of a strong north–south gradient of both subsoil temperature and active-layer thickness that generally matches observations (Beer et al., 2013).

By calculating the active layer depth for each carbon pool and in each latitudinal band, we can determine the fraction of permafrost carbon below the active layer and therefore the amount of organic matter perennially frozen under our baseline climate conditions (i.e. pre-industrial climate). Large amounts of organic matter in permafrost soils reside in the active layer and were affected by past decomposition and release over millennia. It is unclear to what extent the quality of this seasonally-thawed organic material will allow extensive microbial decay in the future. Therefore we follow a strategy similar to Burke et al. (2012) and Harden et al. (2012) of considering only the part of permafrost carbon which was locked in perennially frozen grounds since pre-industrial times and thus was not part of the active carbon cycle for millennia. We hereby assume that our carbon inventory describes organic matter in continuous and discontinuous permafrost. This carbon is likely to represent organic matter perennially frozen since pre-industrial climate. We do not consider soil carbon stored in younger permafrost deposits (sporadic and isolated patches) which likely had been thawed for the majority of the Holocene and therefore is likely depleted in labile organic matter. When accounting for uncertainty in model parameters, we infer a range of about 400 to 1100 Pg of carbon perennially frozen under pre-industrial climate. By combining field information with modelling, Harden et al. (2012) have estimated a total of about 130 to 1060 Pg of carbon perennially frozen under present day climate.

Further, we account for the fact that a large part of the permafrost carbon inventory (i.e. the passive pool) will likely be recalcitrant to decay on a multi-centennial timescale (Schmidt et al., 2011). Assuming a passive pool fraction of about 40 to 70 %, only about 120 to 660 Pg of permafrost carbon can become vulnerable for eventual carbon release in our simulation setting.

To capture uncertainty in modelled carbon fluxes from thawing permafrost deposits, we have independently sampled a set of 18 key model parameters who are subject to

BGD
11, 16599–16643, 2014

either observational or to model description uncertainty. For each warming scenario, we have performed 500 ensemble runs by applying a statistical Monte Carlo sampling and by assuming uniformly and independently distributed model parameters and initial values.

2.3 Permafrost thaw and carbon release

With increasing high latitude warming the active layer will deepen. We model this process by assuming that climate-driven long-term thaw rates can be described depending on four key factors: physical ground properties, mean annual ground temperatures, depth of the thawed sediment layer, and magnitude of the warming anomaly which drives permafrost degradation (see the Supplement). Hereby we capture factors which strongly affect pool-specific thaw dynamics, e.g. talik formation under thermokarst lakes, dampening of the thaw signal with depth, variable soil-ice contents. We therefore can determine the amount of newly thawed organic matter under various anthropogenic emission scenarios as a consequence of warming above pre-industrial temperatures. We hereby assume carbon emissions proportional to the amount of newly thawed carbon in each pool. Eventual carbon emission as CO_2 or CH_4 is determined through calculated aerobic and anaerobic emission rates (see the Supplement).

Finally, the permafrost model was coupled to a simple multi-pool climate-carbon cycle model to close the feedback loop: while the permafrost model simulates permafrost degradation and subsequent carbon release (as CO_2 and CH_4), the climate carbon-cycle model calculates atmospheric changes in CO_2 and CH_4 concentrations and subsequent increases in global mean surface air temperatures. Based on state-of-the-art climate models (CMIP-5, Taylor et al., 2011), we infer polar amplification factors to describe surface air warming in each latitudinal band which then drives permafrost degradation in the next time step.

BGD
11, 16599–16643, 2014

2.4 Model limitations

Our approach of modelling permafrost thaw relies on the simplifying assumption that the main driver of permafrost degradation is the rise of Arctic air temperatures. Yet soil thermal conditions can be influenced by factors other than temperature (e.g. vegetation cover, snow thickness, topography) (Jafarov et al., 2012; Jorgenson et al., 2010). We motivate our modelling approach by focusing on the large-scale and long-term deepening of active layer thickness under various warming scenarios. Although snow cover is considered a key factor for simulating present day permafrost extent consistent with observations (Koven et al., 2013a; Langer et al., 2013; Osterkamp, 2007; Stieglitz et al., 2003), it is unclear how strongly future changes in high-latitude snow cover will affect permafrost degradation. Given that no high-quality data products are available for a circumarctic mapping of snow cover, snow depth, and snow density – and given that climate models simulate strongly divergent pathways of future snowfall – we here make the simplifying assumption that the long term evolution of permafrost is largely driven by changes in surface air temperatures. Similarly, our simplified approach of describing thermokarst dynamics is based on the assumption that future thermokarst formation is largely affected by increasing surface air temperature. Temperature-unrelated, local factors (such as topography, precipitation changes or wildfire) can also be key determinants for thermokarst dynamics. We understand our approach mainly as quantifying carbon fluxes under different hypotheses of future thermokarst development rather than providing deterministic and explicit predictions of individual thermokarst terrains. An alternative scenario of a reduction in high-latitude inland water surface area under future warming was e.g. investigated by Krinner and Boike (2010).

Nutrient limitation in the soils and abrupt carbon release after wildfires are considered two further, potentially important mechanisms for the carbon balance of thawed permafrost deposits which we do not consider in our model design (Mack et al., 2004; Turetsky et al., 2011). Probably the largest effect of unaccounted processes on our simulated carbon fluxes comes from the omission of high latitude vegetation

BGD
11, 16599–16643, 2014

dynamics. Increased carbon uptake in a warmer climate through more productive vegetation can strongly affect the Arctic carbon balance (Schaphoff et al., 2013). The capturing of this feedback component requires the implementation of a dynamic vegetation model which is beyond the scope of this study. Also of importance in this respect is the potential restoration of carbon sinks after lake drainage which could, on the long-term, partially compensate for high CH_4 emission (van Huissteden and Dolman, 2012; Kessler et al., 2012; Jones et al., 2012; Walter Anthony et al., 2012).

Our simulated wetland CH_4 fluxes describe methane produced from newly thawed permafrost carbon. Yet the full carbon balance of wetlands is rather complex and possibly more affected by future changes in soil moisture, soil temperature, and vegetation composition than by the delivery of newly thawed organic matter through permafrost degradation (Olefeldt et al., 2013). The accounting of these additional factors requires the implementation of comprehensive wetland models (such as suggested by Frolking et al., 2001; Kleinen et al., 2012; Eliseev et al., 2008).

3 Model results

3.1 Permafrost degradation

We have run our model under various scenarios of future warming, ranging from moderate (RCP2.6) to extensive (RCP8.5). Under RCP2.6, global greenhouse gas emissions peak by 2020 and decline strongly afterwards. We simulate subsequent increases in global mean surface–air temperatures which are constrained to below two degrees above pre-industrial levels. In case of unmitigated climate change (RCP8.5), global mean surface air temperatures continuously increase and reach 10 °C by the end of the 23rd century at the upper range of our simulations. This pronounced difference in simulated surface air temperatures results in strongly differing pathways of long-term permafrost degradation (Fig. 2).

BGD
11, 16599–16643, 2014

Depending on initial mean annual ground temperatures (MAGTt0), we exemplarily infer for cold (MAGTt0 = −10 °C), medium (MAGTt0 = −5 °C), and warm (MAGTt0 = −0.5 °C) permafrost mean active layer depths of 20, 70, and 250 cm, respectively. In a recent study, Koven et al. (2013a) have diagnosed observed active layer depths north of 55° N from a circumpolar and a Russian data set (CALM, Brown et al., 2000; Zhang et al., 2006). Their analysis suggests a range of measured present-day active layer depths ranging from 30 to 230 cm. The authors underline the challenge of comparing modeled with observed active layer depths given the different spatial coverage of models and observations.

As projections of surface air temperatures only start to diverge strongly after mid of the 21st century, continuous but slow deepening of the active layer is similar under RCP2.6 and RCP8.5 until 2050 (Fig. 2). We first focus on active layer deepening of the largest pool of permafrost carbon, i.e. organic matter in mineral soils under aerobic conditions (Fig. 2, upper panels). Under moderate warming (RCP2.6), active layer depths stabilize after 2100 for cold and medium permafrost temperatures (blue and green curves). Yet permafrost in southerly warm regions will degrade in our simulations with disappearance of near-surface (0 to 3 m) permafrost before 2100 (red curve). Under strong warming (RCP8.5), a sharp increase in thawing rates in the second half of the 21st century can be seen and the majority of model runs suggest a degradation of near-surface permafrost towards the end of the century. In northern and cold permafrost regions, a complete disappearance of near-surface permafrost is only realized after 2150 (blue curve, upper right panel). The sustained long-term warming leads to a continuous deepening of the permafrost table which can reach about 10 m (~ 7 to 13 m, 68 % range) by the year 2300 in our simulations.

Under wetland conditions (i.e. water/ice-saturated sediments), the active layer shows a similar but slower deepening in response to rising surface air temperatures (Fig. 2, mid panels). In contrast, when considering thermokarst lake formation, thaw rates increase sharply (Fig. 2, lower panels). In the first years after intense thermokarst formation, sub-lake talik progression is very pronounced and annual thaw rates amount

BGD
11, 16599–16643, 2014

many decimetres (see the Supplement) – in line with observational and modelling studies (Ling et al., 2012; Kessler et al., 2012) The abrupt thaw dynamics results in disappearance of near-surface permafrost well before 2050 (Fig. 2, lower panels). By the year 2100, typical talik depths amount to 10 to 15 m. The evolution of active layer depths in thermokarst-affected deposits does not strongly differ between moderate and extensive warming (Fig. 2, lower panels). This is because the degradation in thermokarst-affected sediments is driven by lake bottom temperatures. Averaged over a full year, lake bottom temperatures do not strongly differ between moderate and strong surface-air warming (see the Supplement).

In our model setting, we explicitly account for permafrost carbon in deep inventories (Yedoma and refrozen thermokarst deposits). By the end of the 23rd century, typical depths of the permafrost table in these carbon- and ice-rich sediments reach about 5 to 9 m under the RCP8.5 scenario if no abrupt thaw is considered (not shown). Thus even under strong surface air warming, our simulations suggest a large part of the deep carbon deposits will remain perennially frozen over the coming centuries if only gradual thaw is considered. In contrast, in most latitudes of ice-rich Yedoma regions which are affected by new thermokarst formation, thaw reaches the maximum model depth of 15 m before 2300.

3.2 Permafrost carbon release

We define permafrost carbon fluxes similar to Burke et al. (2012) and Harden et al. (2012) as the release from newly thawed permafrost carbon, i.e. the contribution of perennially frozen soil organic matter which becomes part of the active carbon cycle if warmed above pre-industrial temperatures. We stress that these fluxes do not describe the full carbon balance of permafrost regions which is also affected by changes in vegetation uptake, new carbon inputs into deeper soil layers, and carbon release from soil surface layers which were already seasonally thawed under pre-industrial climate (see discussion in Sect. 2.2).

BGD
11, 16599–16643, 2014

Depending on the degree of ground warming and thus on the extent of active layer deepening, differing amounts of newly thawed carbon will be made available for microbial decomposition and eventual release to the atmosphere. Figure 3 illustrates permafrost carbon thaw and emissions under a scenario of moderate warming (RCP2.6, upper panels) and extensive warming (RCP8.5, lower panels). Under RCP2.6, largest increases in newly thawed permafrost carbon (Fig. 3, first column) are realized until mid of the 21st century with a total of 167 Pg-C (113–239 Pg-C, 68 % range) of which 40–70 % is assumed part of the passive carbon pool and thus recalcitrant on the timescale considered here. In contrast, the pronounced and continuous warming under RCP8.5 results in much larger amounts of newly thawed permafrost carbon. By the year 2100, 367 Pg-C are thawed (233 to 497 Pg-C, 68 % range), and through further permafrost degradation in the 22nd and 23rd century, a total of 564 Pg-C (392 to 734 Pg-C, 68 % range) of organic matter is newly thawed by the year 2300. Focusing on the top three soil meters and considering a larger uncertainty spread in the permafrost carbon inventory, two recent studies estimated a min-max range of 75–870 Pg (Burke et al., 2012) and of 105 to 851 Pg (Harden et al., 2012) of newly thawed permafrost carbon under RCP8.5 until the year 2100.

The intensity of carbon release after permafrost thaw differs strongly among the scenarios in our simulations (Fig. 3). While under RCP2.6, maximum annual CO_2 emission rates are constrained to about 0.4 Pg-C yr^{-1} (0.2 to 0.6, 68 % range), peak emission rates under RCP8.5 amount to 1.7 Pg-C yr^{-1} (median) and can reach 2.6 Pg-C yr^{-1} (upper 68 % range). The decline in emission rates in the 22nd and 23rd century describes the depletion of thawed permafrost carbon through release to the atmosphere. Under all RCPs, peak CO_2 emission rates occur around the end of the 21st century.

Due to much lower anaerobic CH_4 as compared to aerobic CO_2 production rates (Table 1), and due to the majority of soil carbon being thawed under aerobic conditions, methane emission from thawing permafrost soils amounts only a few percent of total permafrost carbon release. Observational and modelling experts have estimated

BGD
11, 16599–16643, 2014

that methane will contribute by about 1.5–3.5 % to future permafrost carbon release (Schuur et al., 2013).

Given the slow progression of permafrost thaw in wetland-affected sediments, CH_4 release from newly thawed permafrost carbon is only discernible after end of this century (Fig. 3). Our simulations suggest maximum annual CH_4 emission rates of a few Tg-CH_4 for moderate warming, about 16 Tg-CH_4 (8–28, 68 % range) for strong warming. To the contrary, abrupt thaw under thermokarst lakes results in peak methane emission after mid of this century. Under RCP2.6, maximum annual CH_4 emissions are constrained to about 5.5 Tg-CH_4 (up to 11.5 for the upper 68 % range), while under RCP8.5 peak CH_4 emission reach about 26 Tg-CH_4 (14–49, 68 % range). The strong decline in emission rates towards the end of the century is an expression of the sharp decrease in thermokarst lake extents through increasing drainage under sustained warming (see Fig. S1 in the Supplement). A pronounced spike in methane emissions as a consequence of rapidly expanding and subsequently shrinking thermokarst lake areas is in line with hypotheses of past rapid thermokarst lake formation and expansion. Walter et al. (2007a) suggest an annual CH_4 release of 30–40 Tg-CH_4 from thermokarst lakes to partially explain CH_4 excursions of early Holocene atmospheric methane levels. Brosius et al. (2012) discuss a yearly contribution from thermokarst lakes of 15 ± 4 Tg-CH_4 during the Younger Dryas and 25 ± 5 Tg-CH_4 during the Preboreal period.

Our modelled total CH_4 fluxes under strong warming are comparable in magnitude to an estimated current release of 24.2 ± 10.5 Tg-CH_4 year^{-1} from northern lakes (Walter et al., 2007b). The majority of our results suggest that methane fluxes from newly thawed permafrost carbon are an order of magnitude smaller than the contribution from all current natural (about 200 Tg-CH_4 yr^{-1}) and anthropogenic (about 350 Tg-CH_4 yr^{-1}) sources (Environmental Protection Agency (EPA), 2010). Focusing on thermokarst lakes in ice-rich sediments (i.e. on our Yedoma and refrozen thermokarst deposits), we infer 21st century averaged median emission rates of 6.3 Tg-CH_4 yr^{-1} which are about double compared to recent model estimates of thermokarst lake CH_4 release

BGD
11, 16599–16643, 2014

(van Huissteden et al., 2011; Gao et al., 2013). Based on a carbon mass balance calculation of methane release from Siberian thermokarst lakes, Walter et al. (2007b) suggest a contribution of about 50 000 Tg-CH_4 (or 50–100 Tg-CH_4 yr^{-1} over centuries) in case of a complete thaw of the Yedoma ice-complex. Considering contributions from permafrost wetlands and lakes, Burke et al. (2012) infer 21st century methane emission rates below 53 Tg-CH_4 yr^{-1} for the majority of their model runs. Although our CH_4 release estimates, which are inferred by an independent modelling approach, are comparable in magnitude with recent work, a direct comparison with studies extrapolating observed CH_4 fluxes should be considered with care. Observed methane fluxes describe the full carbon balance, including contributions from soil surface layers and vegetation cover, which we do not consider in our model setting.

Under strong warming, our modelled methane emissions accumulate to 836 to 2614 Tg-CH_4 (68 % range) until the year 2100. Maximum contributions until the year 2300 can reach 10.000 Tg-CH_4 (upper 68 % range, see Table 2).

We have additionally analysed the impact of uncertainty in initial MAGT distribution on the calculated carbon fluxes. Soil temperatures affect the magnitude of carbon release in two ways. First, MAGTs determine the initial active layer profile and thus the amount of carbon perennially frozen under per-industrial climate. Second, soil temperatures determine the vulnerability of permafrost carbon to future degradation. Based on a model ensemble with sampling solely uncertainty in MAGT, we inferred a spread in the year 2100 of 32.5 ± 23 % Pg-C and 81.5 ± 8 % Pg-C for the scenarios RCP2.6 and RCP8.5 respectively, which further increase to 60 ± 33 % Pg-C and 235 ± 6 % Pg-C in the year 2300.The factor 3–5 larger fractional uncertainty for the climate mitigation scenario (RCP2.6) illustrates the enhanced sensitivity to initial permafrost temperatures of modelled carbon fluxes under moderate warming.

3.3 Contribution of deep deposits

We account for a total of 230 Pg of organic matter buried below 3 m in Yedoma and refrozen thermokarst deposits (including taberal sediments). Under aerobic or wetland

BGD
11, 16599–16643, 2014

conditions, our simulations suggest only small contributions of these deep deposits to the total release of newly thawed permafrost carbon even under scenarios of strong warming (Fig. 4). Discernible contributions are only inferred towards the end of our simulations (23rd century), with fluxes from deep deposits contributing a maximum of about 10 % to accumulated CO_2 release or about 5 % to total wetland CH_4 release (upper 68 % ranges). The lagged response of deep carbon release is an expression of the slow penetration of heat into the ground. In most latitude bands under the RCP2.6 scenario, no frozen carbon from deep deposits is thawed as the moderate warming does not result in active layer depths exceeding three meters.

Yet if abrupt thaw under thermokarst lakes is accounted for, the fast propagation of sub-lake taliks can unlock large amounts of perennially frozen deep organic matter even within this century. Our simulations suggest that until 2100 about 25–30 % of emitted methane from thermokarst lakes stems from contributions of deep permafrost carbon (Fig. 4, lower panel). Maximum contributions until 2300 can amount to 35 % (upper 68 % range).

3.4 Permafrost-affected warming

To disentangle the warming caused by anthropogenic greenhouse gas emission from warming caused by permafrost-carbon release, we have performed paired-simulations under identical parameter settings – once with the permafrost module activated and once deactivated. The difference in global mean surface-air temperatures between each pair of ensemble simulations is what we define as the additional global warming caused by newly thawed permafrost carbon (i.e. permafrost-affected warming).

Although permafrost carbon release increases strongly with rising global temperatures (Fig. 3), our results suggest a permafrost-affected global warming of about 0.05–0.15 °C (68 % range) until 2100 which is only slightly dependent on the anthropogenic emission pathway. The quasi path-independency of the permafrost temperature feedback is an expression of the decreasing radiative efficiency under high atmospheric greenhouse gas levels. Long-term warming from the release of newly

BGD
11, 16599–16643, 2014

thawed permafrost carbon can add an additional 0.4 °C (upper 68 % range) to global temperatures until the year 2300. Despite of methane release contributing only a few percent to total permafrost carbon release, our analyses suggest that it can cause up to about 40 % (upper 68 % range) of permafrost-affected warming. In the 22nd and 23rd century the radiative balance is largely affected by aerobic permafrost carbon release as emitted CO_2 accumulates over centuries in the atmosphere – in contrast to the fast decline in methane anomalies with a typical CH_4 life-time of about a decade.

4 Discussion and conclusions

This paper presents a new observation-based model for assessing long-term climatic consequences of permafrost degradation. Our simulation strategy consisted in partitioning carbon inventories into different pools of varying soil and surface conditions to model site-specific carbon release. Rather than trying to capture permafrost-carbon dynamics in detail, we instead have aimed at describing in a simplified manner a multitude of processes which are key to permafrost carbon release – such as abrupt thaw in thermokarst-affected sediments. We have especially aimed at accounting for the contribution of carbon release from known deep deposits in the 1.3 million km^2 large Yedoma region of Siberia and Alaska (Strauss et al., 2013; Walter Anthony et al., 2014), which had been neglected in most previous modelling studies. Our computationally efficient model has enabled us to scan the large uncertainty inherent to observing and modelling the permafrost carbon feedback. In our study we had focused on the contribution of newly thawed permafrost carbon which becomes vulnerable through soil warming above pre-industrial temperatures. However, we stress that the full permafrost carbon feedback is also affected by contributions from soil surface layers (seasonally thawed active layer) and changes in high-latitude vegetation which are not considered in this study.

The large spread in future carbon release from permafrost degradation inferred from modelling studies (see Schaefer et al., 2014 for an overview) is caused by

BGD
11, 16599–16643, 2014

various factors. One key issue are pronounced differences in the strength of simulated permafrost degradation. In a recent observationally-constrained model study, Hayes et al. (2014) suggest a mean deepening of the active layer of 6.8 cm over the period 1970 to 2006. We simulate a deepening by 5.9–15.5 cm (68 % range) over the same period when focusing on our mineral soil pool under aerobic conditions. By the year 2100, our simulations suggest a mean active layer deepening of this pool by 40–76 cm under RCP2.6, and of 105–316 cm under RCP8.5. The latter range covers a large part of previous estimates, although some studies suggest lower values (Schaefer et al., 2014). Yet a comparison of aggregated simulated active layer depths should be considered with care as differences in definitions (e.g. of the considered permafrost domain and its vertical extent) or different assumptions of future warming can lead to estimating systematically lower or higher active layer depths.

Our simulations suggest that permafrost emissions will be strongly constrained when limiting global warming: under a climate mitigation pathway (RCP2.6), the increase in high latitude temperatures results in a moderate deepening of the active layer which stabilizes in most latitudes after the year 2100 (in line with diagnostics based on complex models, Slater and Lawrence, 2013). Until end of the century about 36 Pg (20–58 Pg, 68 % range) of carbon can be released as CO_2. Under strong warming (RCP8.5), permafrost degradation proves substantial and cumulated CO_2 emissions can reach 87 Pg-C (42–141 Pg-C, 68 % range) by the year 2100. A release of 87 Pg-C corresponds to a mean loss of about 12 % of our initial inventory of 750 Pg of carbon perennially frozen under pre-industrial climate. Modelling studies estimated a loss of 6–33 % of initial permafrost carbon stocks, while the majority of models suggest a loss of 10–20 % (Schaefer et al., 2014). Incubation of permafrost soil samples suggest a carbon loss from mineral soils under aerobic conditions of 13 and 15 % over 100 years when assuming thaw during 4 months in a year (Schädel et al., 2013; Knoblauch et al., 2013).

The sustained long-term warming under RCP8.5 results in an almost complete degradation of near-surface permafrost in the 22nd century and illustrates the long-

BGD
11, 16599–16643, 2014

term consequences of permafrost carbon release: our simulations suggest that until the year 2300, a total of about 157–313 Pg-C can be released to the atmosphere. Peak emissions occur at the end of the 21st century and reach 2.5 Pg-C per year under strong warming (RCP8.5, upper 68 % range). In the 22nd and 23rd century depletion of permafrost carbon gets increasingly noticeable and total emissions from newly thawed carbon decline. Our analyses have shown a large potential of reducing uncertainty in simulated carbon fluxes especially for climate mitigation pathways when more and spatially higher resolved data of present day permafrost temperatures will be available.

Based on our conceptual model of thermokarst lake formation and drainage, our results suggest that abrupt thaw can unlock large amounts of frozen carbon within this century. We infer a deepening of the permafrost table by several meters in 100 years after thermokarst initiation, with additional talik propagation large enough to fully thaw sediments to our lower pool boundary (15 m) in the second half of the 22nd century. Subsequent CH_4 release from newly thawed permafrost under RCP8.5 results in peak emissions up to about 50 Tg-CH_4 yr^{-1} (upper 68 % range) in the 21st century. Our modelled methane releases are of a magnitude comparable to paleo-based estimates from past thermokarst dynamics (Walter et al., 2007a; Brosius et al., 2012) and suggest slightly larger fluxes compared to two recent modelling studies (Gao et al., 2013; van Huissteden et al., 2011). In contrast to abrupt thaw and fast release under thermokarst lakes, methane release from newly thawed carbon in wetland-affected soils is slow with discernible contributions only in the 22nd and 23rd century. Although contributing only a few percent to total permafrost carbon release, our simulated methane fluxes from newly thawed permafrost carbon can cause up to 40 % of permafrost-affected warming in the 21st century. Given the short lifetime of methane, the radiative forcing from permafrost carbon in the 22nd and 23rd century is largely dominated by aerobic CO_2 release.

Under strong warming, our modelled methane emissions from newly thawed permafrost accumulate to some thousand terra grammes until the year 2100, with maximum contributions of 10 000 Tg-CH_4 (upper 68 % range) until the year 2300

BGD
11, 16599–16643, 2014

(see Table 1). Yet the release of this amount of CH_4 would only slightly affect future atmospheric methane levels under projected RCP CH_4 emissions as the anthropogenic contribution will dominate atmospheric CH_4 concentrations. In the extremely unlikely case of a complete thaw of the Yedoma ice-complex, Walter et al. (2007b) have discussed a contribution of 50 000 Tg of methane being released into the atmosphere.

To put into relation the contribution of carbon fluxes from deep deposits to the total, circumpolar release from newly thawed permafrost, we have analysed the contribution of individual pools. Our simulations suggest that the omission of deep carbon stores is unlikely to strongly affect CO_2 release from permafrost degradation in the coming centuries. In contrast, CH_4 fluxes from newly thawed permafrost are strongly influenced by carbon release from organic matter stored in deep deposits. Although our considered deep pools cover only about 12 % of the total area of Northern Hemisphere gelisols, and despite of the organic matter in these pools being buried deep in the ground, these pools contribute significantly to the total CH_4 balance because abrupt thaw under thermokarst lakes can unlock a large portion of previously inert organic matter. About a quarter of 21st century CH_4 release stems from newly thawed organic matter stored in deep deposits (i.e. from soil layers deeper than 3 m). Further, our analyses revealed that the release from mineralization of labile organic matter contributes disproportionately high to these fluxes. Despite of assuming a fast (labile) pool fraction of only a few percent, our simulated CH_4 fluxes from newly thawed labile organic matter account for up to half of the total thermokarst-affected deep CH_4 release in the 21st century. Therefore, improved observational estimates of the share of labile organic matter would help to reduce uncertainty in simulated methane release from deep carbon deposits (Strauss et al., 2014). The analysis of individual deep pools revealed a methane release about a factor of two larger from refrozen thermokarst compared to unaltered Yedoma.

Our results suggest a mean increase in global average surface temperature of about 0.1 °C by the year 2100 (0.03–0.14 °C, 68 % ranges) caused by carbon release from newly thawed permafrost soils. Long-term warming through the permafrost carbon

BGD
11, 16599–16643, 2014

feedback (year 2300) can add an additional 0.4 °C (upper 68 % range) to projected global mean surface air temperatures. Our analyses suggest a permafrost-affected warming which is similar under differing scenarios of anthropogenic emissions – despite of largest carbon release from permafrost degradation under strong warming. The weak path dependency is a consequence of the decreasing radiative efficiency of emitted permafrost carbon under increasing greenhouse gas levels. MacDougall et al. (2012) also modelled a permafrost-carbon feedback largely independent of the emission pathway but inferred larger upper estimates of permafrost-affected warming due to considering a much larger pool available for carbon release triggered by permafrost degradation. An increase in the permafrost temperature feedback with global warming was inferred by Burke et al. (2012) who considered a much larger spread in the near-surface permafrost carbon inventory (∼ 300 to 1800 Pg-C) and who estimated the permafrost temperature feedback by the year 2100 as 0.02–0.11 °C and 0.08–0.36 °C (90 % ranges) under RCP2.6 and RCP8.5 respectively.

5 Outlook

We consider our estimates conservative because carbon release from further, in this study unaccounted sources, are likely to increase the strength of the full permafrost-carbon feedback.

Firstly, our study focuses solely on the carbon fluxes resulting from newly thawed soils and deposits in our simulation scenarios, thus excluding carbon fluxes from permafrost-affected soils in the current active layer. These soils will also warm to different levels under RCP scenarios and very likely will be subject to enhanced mineralization of the large already seasonally thawed C pool of about 500 Pg (Hugelius et al., 2014). Secondly, we do not account for the contribution of newly thawed organic matter of low quality, which we assume recalcitrant on the timescale considered here (i.e. 40–70 % of thawed organic matter is not available for release). More data and longer time series of incubation experiments, in combination with modelling

BGD
11, 16599–16643, 2014

work of soil-carbon dynamics, are needed to better constrain timescale assumptions for soil organic matter decomposition. Also of importance are improved data-based estimates of $CH_4:CO_2$ anaerobic production ratios, which determine the share of carbon emitted as CH_4. Thirdly, we do not account for the presence, and potential thaw and mobilization, of deep frozen carbon outside the Yedoma and RTK region. Currently no coherent data is available on the distribution and organic carbon characteristics of soils and sediments below 3 m depth for large regions in Siberia, Alaska, and Canada. Our model results suggest that these depths will be affected by thaw over the coming centuries and available thawed organic matter would contribute to the permafrost carbon feedback. Fourthly, we do not consider carbon release from degrading submarine permafrost which might result in an underestimation of circumpolar permafrost-affected methane fluxes in our study (Shakhova et al., 2010). Fifthly, extensive permafrost degradation can support a large and abrupt release of fossil CH_4 from below the permafrost cap based on presence of regional hydrocarbon reservoirs and geologic pathways for gas migration (Walter Anthony et al., 2012). We do not consider this pathway of abrupt methane release which could lead to a non-gradual increase in the permafrost-carbon feedback if sub-cap CH_4 increases non-linearly with warming. Likely, the most important omission in our study stems from changes in the high-latitude carbon balance caused by altered vegetation dynamics. Here, an increased carbon uptake through more productive high-latitude vegetation and the renewal of carbon sinks in drained thermokarst basins can considerably decrease the net carbon loss on centennial time-scales (Schaphoff et al., 2013; van Huissteden et al., 2011). Yet this loss can be partially compensated through enhanced respiration of soil-surface organic matter which is stored in large amounts in permafrost regions (but which was not incorporated into permafrost in the past and thus is not considered in this study here). On the other hand, a transition from tundra- towards taiga-dominated landscapes as a consequence of high-latitude warming can strongly decrease surface albedo and therefore additionally warm permafrost regions. We consider the implementation of high-latitude vegetation dynamics into permafrost

BGD
11, 16599–16643, 2014

models a key step towards an improved capturing of the timing and strength of the full permafrost-carbon feedback.

The Supplement related to this article is available online at doi:10.5194/bgd-11-16599-2014-supplement.

Acknowledgements. Special thanks to S. Mathesius for the analysis of CMIP-5 data, G. Hugelius for providing soil carbon data for near-surface permafrost inventories, M. Allen for having provided an earlier version of the climate carbon cycle model, H. Lantuit for discussing aspects of permafrost degradation through coastal erosion, C. Schädel for discussing incubation results of soil carbon lability, and Katey Walter Anthony and Hanna Lee for discussing ratios of methane vs. carbon dioxide production rates.

Portions of this study were supported by the Federal Environment Agency for Germany (UBA) under project UFOPLAN FKZ 3712 41 106 and ERC Starting Grant #338 335.

J. Strauss was supported by a grant of the Studienstiftung des Deutschen Volkes (German National Academic Foundation) and the German Federal Ministry of Education and Research (Grant 01DM12011).

References

Abnizova, A., Siemens, J., Langer, M., and Boike, J.: Small ponds with major impact: the relevance of ponds and lakes in permafrost landscapes to carbon dioxide emissions, Global Biogeochem. Cy., 26, GB2041, doi:10.1029/2011GB004237, 2012.

Arp, C. D., Jones, B. M., Lu, Z., and Whitman, M. S.: Shifting balance of thermokarst lake ice regimes across the Arctic Coastal Plain of northern Alaska, Geophys. Res. Lett., 39, L16503, doi:10.1029/2012GL052518, 2012.

Avis, C. A., Weaver, A. J., and Meissner, K. J.: Reduction in areal extent of high-latitude wetlands in response to permafrost thaw, Nat. Geosci., 4, 444–448, 2011.

Beer, C., Fedorov, A. N., and Torgovkin, Y.: Permafrost temperature and active-layer thickness of Yakutia with 0.5-degree spatial resolution for model evaluation, Earth Syst. Sci. Data, 5, 305–310, doi:10.5194/essd-5-305-2013, 2013.

Boike, J., Langer, M., Lantuit, H., Muster, S., Roth, K., Sachs, T., Overduin, P., Westermann, S., and McGuire, A. D.: Permafrost – physical aspects, carbon cycling, databases and uncertainties, in: Recarbonization of the Biosphere, edited by: Lal, R., Lorenz, K., Hüttl, R. F., Schneider, B. U., and von Braun, J., Springer, Dordrecht, Netherlands, 159–185, 2012.

Boike, J., Kattenstroth, B., Abramova, K., Bornemann, N., Chetverova, A., Fedorova, I., Fröb, K., Grigoriev, M., Grüber, M., Kutzbach, L., Langer, M., Minke, M., Muster, S., Piel, K., Pfeiffer, E.-M., Stoof, G., Westermann, S., Wischnewski, K., Wille, C., and Hubberten, H.-W.: Baseline characteristics of climate, permafrost and land cover from a new permafrost observatory in the Lena River Delta, Siberia (1998–2011), Biogeosciences, 10, 2105–2128, doi:10.5194/bg-10-2105-2013, 2013.

Brosius, L. S., Walter Anthony, K. M., Grosse, G., Chanton, J. P., Farquharson, L. M., Overduin, P. P., and Meyer, H.: Using the deuterium isotope composition of permafrost meltwater to constrain thermokarst lake contributions to atmospheric CH_4 during the last deglaciation, J. Geophys. Res.-Biogeosci., 117, G01022, doi:10.1029/2011JG001810, 2012.

Brown, J., Hinkel, K. M., and Nelson, F. E.: The circumpolar active layer monitoring (calm) program: research designs and initial results, Polar Geography, 24, 166–258, 2000.

Burke, E. J., Hartley, I. P., and Jones, C. D.: Uncertainties in the global temperature change caused by carbon release from permafrost thawing, The Cryosphere, 6, 1063–1076, doi:10.5194/tc-6-1063-2012, 2012.

Conrad, R., Klose, M., and Claus, P.: Pathway of CH_4 formation in anoxic rice field soil and rice roots determined by 13C-stable isotope fractionation, Chemosphere, 47, 797–806, doi:10.1016/S0045-6535(02)00120-0, 2002.

Dankers, R., Burke, E. J., and Price, J.: Simulation of permafrost and seasonal thaw depth in the JULES land surface scheme, The Cryosphere, 5, 773–790, doi:10.5194/tc-5-773-2011, 2011.

Dutta, K., Schuur, E. A. G., Neff, J. C., and Zimov, S. A.: Potential carbon release from permafrost soils of Northeastern Siberia, Glob. Change Biol., 12, 2336–2351, 2006.

Ekici, A., Beer, C., Hagemann, S., Boike, J., Langer, M., and Hauck, C.: Simulating high-latitude permafrost regions by the JSBACH terrestrial ecosystem model, Geosci. Model Dev., 7, 631–647, doi:10.5194/gmd-7-631-2014, 2014.

Eliseev, A. V., Mokhov, I. I., Arzhanov, M. M., Demchenko, P. F., and Denisov, S. N.: Interaction of the methane cycle and processes in wetland ecosystems in a climate model of intermediate complexity, Izv. Atmos. Oceanic Phy., 44, 139–152, 2008.

Environmental Protection Agency (EPA): Methane and nitrous oxide emissions from natural sources EPA 430-R-10-001, US Environmental Protection Agency, Washington, DC, 2010.

Frauenfeld, O. W., Zhang, T., Barry, R. G., and Gilichinsky, D.: Interdecadal changes in seasonal freeze and thaw depths in Russia, J. Geophys. Res.-Atmos., 109, D05101, doi:10.1029/2003JD004245, 2004.

Friedlingstein, P., Cox, P., Betts, R., Bopp, L., von Bloh, W., Brovkin, V., Cadule, P., Doney, S., Eby, M., Fung, I., Bala, G., John, J., Jones, C., Joos, F., Kato, T., Kawamiya, M., Knorr, W., Lindsay, K., Matthews, H. D., Raddatz, T., Rayner, P., Reick, C., Roeckner, E., Schnitzler, K.-G., Schnur, R., Strassmann, K., Weaver, K., Yoshikawa, C., and Zeng, N.: Climate–carbon cycle feedback analysis: results from the C4MIP model intercomparison, J. Climate, 19, 3337–3353, doi:10.1175/JCLI3800.1, 2006.

Frolking, S., Roulet, N. T., Moore, T. R., Richard, P. J. H., Lavoie, M., and Muller, S. D.: Modeling northern peatland decomposition and peat accumulation, Ecosystems, 4, 479–498, 2001.

Gao, X., Schlosser, C. A., Sokolov, A., Anthony, K. W., Zhuang, Q., and Kicklighter, D.: Permafrost degradation and methane: low risk of biogeochemical climate-warming feedback, Environ. Res. Lett., 8, 035014, doi:10.1088/1748-9326/8/3/035014, 2013

Gouttevin, I., Menegoz, M., Dominé, F., Krinner, G., Koven, C., Ciais, P., Tarnocai, C., and Boike, J.: How the insulating properties of snow affect soil carbon distribution in the continental pan-Arctic area, J. Geophys. Res.-Biogeosci., 117, G02020, doi:10.1029/2011JG001916, 2012.

Grosse, G., Schirrmeister, L., Siegert, C., Kunitsky, V. V., Slagoda, E. A., Andreev, A. A., and Dereviagyn, A. Y.: Geological and geomorphological evolution of a sedimentary periglacial landscape in Northeast Siberia during the Late Quaternary, Geomorphology, 86, 25–51, doi:10.1016/j.geomorph.2006.08.005, 2007.

Grosse, G., Harden, J., Turetsky, M., McGuire, A. D., Camill, P., Tarnocai, C., Frolking, S., Schuur, E. A. G., Jorgenson, T., Marchenko, S., Romanovsky, V., Wickland, K. P., French, N., Waldrop, M., Bourgeau-Chavez, L., and Striegl, R. G.: Vulnerability of high-latitude soil organic carbon in North America to disturbance, J. Geophys. Res., 116, G00K06,doi:10.1029/2010JG001507, 2011.

BGD
11, 16599–16643, 2014

Observation-based modelling of permafrost carbon fluxes

T. Schneider von Deimling et al.

Harden, J. W., Koven, C. D., Ping, C.-L., Hugelius, G., David McGuire, A., Camill, P., Jorgenson, T., Kuhry, P., Michaelson, G. J., O'Donnell, J. A., Schuur, E. A. G., Tarnocai, C., Johnson, K., and Grosse, G.: Field information links permafrost carbon to physical vulnerabilities of thawing, Geophys. Res. Lett., 39, L15704, doi:10.1029/2012GL051958, 2012.

Hayes, D. J., Kicklighter, D. W., McGuire, A. D., Chen, M., Zhuang, Q., Yuan, F., Melillo, J. M., and Wullschleger, S. D.: The impacts of recent permafrost thaw on land–atmosphere greenhouse gas exchange, Environ. Res. Lett., 9, 045005, doi:10.1088/1748-9326/9/4/045005 2014.

Hugelius, G., Tarnocai, C., Broll, G., Canadell, J. G., Kuhry, P., and Swanson, D. K.: The Northern Circumpolar Soil Carbon Database: spatially distributed datasets of soil coverage and soil carbon storage in the northern permafrost regions, Earth Syst. Sci. Data, 5, 3–13, doi:10.5194/essd-5-3-2013, 2013.

Hugelius, G., Strauss, J., Zubrzycki, S., Harden, J. W., Schuur, E. A. G., Ping, C. L., Schirrmeister, L., Grosse, G., Michaelson, G. J., Koven, C. D., O'Donnell, J. A., Elberling, B., Mishra, U., Camill, P., Yu, Z., Palmtag, J., and Kuhry, P.: Improved estimates show large circumpolar stocks of permafrost carbon while quantifying substantial uncertainty ranges and identifying remaining data gaps, Biogeosciences Discuss., 11, 4771–4822, doi:10.5194/bgd-11-4771-2014, 2014.

Jafarov, E. E., Marchenko, S. S., and Romanovsky, V. E.: Numerical modeling of permafrost dynamics in Alaska using a high spatial resolution dataset, The Cryosphere, 6, 613–624, doi:10.5194/tc-6-613-2012, 2012.

Jones, B. M., Grosse, G., Arp, C. D., Jones, M. C., Walter Anthony, K. M., and Romanovsky, V. E.: Modern thermokarst lake dynamics in the continuous permafrost zone, northern Seward Peninsula, Alaska, J. Geophys. Res.-Biogeosci., 116, G00M03, doi:10.1029/2011JG001666, 2011.

Jones, M. C., Grosse, G., Jones, B. M., and Walter Anthony, K.: Peat accumulation in drained thermokarst lake basins in continuous, ice-rich permafrost, northern Seward Peninsula, Alaska, J. Geophys. Res.-Biogeosci., 117, G00M07, doi:10.1029/2011JG001766, 2012.

Jorgenson, M. T., Shur, Y. L., and Pullman, E. R.: Abrupt increase in permafrost degradation in Arctic Alaska, Geophys. Res. Lett., 33, L02503, doi:10.1029/2005GL024960, 2006.

BGD
11, 16599–16643, 2014

Jorgenson, M. T., Romanovsky, V., Harden, J., Shur, Y., O'Donnell, J., Schuur, E. A. G., Kanevskiy, M., and Marchenko, S.: Resilience and vulnerability of permafrost to climate change, Can. J. Forest Res., 40, 1219–1236, 2010.

Kaufman, D. S., Ager, T. A., Anderson, N. J., Anderson, P. M., Andrews, J. T., Bartlein, P. J., Brubaker, L. B., Coats, L. L., Cwynar, L. C., Duvall, M. L., Dyke, A. S., Edwards, M. E., Eisner, W. R., Gajewski, K., Geirsdóttir, A., Hu, F. S., Jennings, A. E., Kaplan, M. R., Kerwin, M. W., Lozhkin, A. V., MacDonald, G. M., Miller, G. H., Mock, C. J., Oswald, W. W., Otto-Bliesner, B. L., Porinchu, D. F., Rühland, K., Smol, J. P., Steig, E. J., and Wolfe, B. B.: Holocene thermal maximum in the western Arctic (0–180° W), Quaternary Sci. Rev., 23, 529–560, doi:10.1016/j.quascirev.2003.09.007, 2004.

Kessler, M. A., Plug, L. J., and Walter Anthony, K. M.: Simulating the decadal- to millennial-scale dynamics of morphology and sequestered carbon mobilization of two thermokarst lakes in NW Alaska, J. Geophys. Res.-Biogeosci., 117, G00M06, doi:10.1029/2011JG001796, 2012.

Khvorostyanov, D. V., Ciais, P., Krinner, G., and Zimov, S. A.: Vulnerability of east Siberia's frozen carbon stores to future warming, Geophys. Res. Lett., 35, L10703,doi:10.1029/2008GL033639, 2008.

Kleinen, T., Brovkin, V., and Schuldt, R. J.: A dynamic model of wetland extent and peat accumulation: results for the Holocene, Biogeosciences, 9, 235–248, doi:10.5194/bg-9-235-2012, 2012.

Knoblauch, C., Beer, C., Sosnin, A., Wagner, D., and Pfeiffer, E. M.: Predicting long-term carbon mineralization and trace gas production from thawing permafrost of Northeast Siberia, Glob. Change Biol., 19, 1160–1172, 2013.

Kokelj, S. V., Lacelle, D., Lantz, T. C., Tunnicliffe, J., Malone, L., Clark, I. D., and Chin, K. S.: Thawing of massive ground ice in mega slumps drives increases in stream sediment and solute flux across a range of watershed scales, J. Geophys. Res.-Earth, 118, 681–692, doi:10.1002/jgrf.20063, 2013.

Koven, C., Friedlingstein, P., Ciais, P., Khvorostyanov, D., Krinner, G., and Tarnocai, C.: On the formation of high-latitude soil carbon stocks: effects of cryoturbation and insulation by organic matter in a land surface model, Geophys. Res. Lett., 36, L21501, doi:10.1029/2009GL040150, 2009.

Koven, C. D., Ringeval, B., Friedlingstein, P., Ciais, P., Cadule, P., Khvorostyanov, D., Krinner, G., and Tarnocai, C.: Permafrost carbon-climate feedbacks accelerate global warming, P. Natl. Acad. Sci. USA, 108, 14769–14774, 2011.

BGD
11, 16599–16643, 2014

Koven, C. D., Riley, W. J., and Stern, A.: Analysis of permafrost thermal dynamics and response to climate change in the CMIP5 Earth System Models, J. Climate, 26, 1877–1900, doi:10.1175/JCLI-D-12-00228.1, 2013a.

Koven, C. D., Riley, W. J., Subin, Z. M., Tang, J. Y., Torn, M. S., Collins, W. D., Bonan, G. B., Lawrence, D. M., and Swenson, S. C.: The effect of vertically resolved soil biogeochemistry and alternate soil C and N models on C dynamics of CLM4, Biogeosciences, 10, 7109–7131, doi:10.5194/bg-10-7109-2013, 2013b.

Krinner, G. and Boike, J.: A study of the large-scale climatic effects of a possible disappearance of high-latitude inland water surfaces during the 21st century, Boreal Environ. Res., 15, 203–217, 2010.

Langer, M., Westermann, S., Heikenfeld, M., Dorn, W., and Boike, J.: Satellite-based modeling of permafrost temperatures in a tundra lowland landscape, Remote Sens. Environ., 135, 12–24, doi:10.1016/j.rse.2013.03.011, 2013.

Laurion, I., Vincent, W. F., MacIntyre, S., Retamal, L., Dupont, C., Francus, P., and Pienitz, R.: Variability in greenhouse gas emissions from permafrost thaw ponds, Limnol. Oceanogr., 55, 115–133, 2010.

Lawrence, D. M. and Slater, A. G.: Incorporating organic soil into a global climate model, Clim. Dynam., 30, 145–160, 2008.

Lawrence, D. M., Oleson, K. W., Flanner, M. G., Thornton, P. E., Swenson, S. C., Lawrence, P. J., Zeng, X., Yang, Z.-L., Levis, S., Sakaguchi, K., Bonan, G. B., and Slater, A. G.: Parameterization improvements and functional and structural advances in Version 4 of the Community Land Model, Journal of Advances in Modeling Earth Systems, 3, M03001, doi:10.1029/2011ms000045, 2011.

Lee, H., Schuur, E. A. G., Inglett, K. S., Lavoie, M., and Chanton, J. P.: The rate of permafrost carbon release under aerobic and anaerobic conditions and its potential effects on climate, Glob. Change Biol., 18, 515–527, doi:10.1111/j.1365-2486.2011.02519.x, 2012.

Ling, F.: Numerical simulation of permafrost thermal regime and talik development under shallow thaw lakes on the Alaskan Arctic Coastal Plain, J. Geophys. Res., 108, 4511–4511, 2003.

Ling, F., Wu, Q., Zhang, T., and Niu, F.: Modelling open-talik formation and permafrost lateral thaw under a thermokarst lake, Beiluhe Basin, Qinghai-Tibet Plateau, Permafrost Periglac., 23, 312–321, doi:10.1002/ppp.1754, 2012.

BGD
11, 16599–16643, 2014

Observation-based modelling of permafrost carbon fluxes

T. Schneider von Deimling et al.

MacDougall, A. H., Avis, C. A., and Weaver, A. J.: Significant contribution to climate warming from the permafrost carbon feedback, Nat. Geosci., 5, 719–721, doi:10.1038/ngeo1573, 2012

Mack, M. C., Schuur, E. A. G., Bret-Harte, M. S., Shaver, G. R., and Chapin, F. S.: Ecosystem carbon storage in arctic tundra reduced by long-term nutrient fertilization, Nature, 431, 440–443, 2004.

Marcott, S. A., Shakun, J. D., Clark, P. U., and Mix, A. C.: A reconstruction of regional and global temperature for the past 11,300 years, Science, 339, 1198–1201, doi:10.1126/science.1228026, 2013.

Mishra, U., Jastrow, J. D., Matamala, R., Hugelius, G., Koven, C. D., Harden, J. W., Ping, C. L., Michaelson, G. J., Fan, Z., Miller, R. M., McGuire, A. D., Tarnocai, C., Kuhry, P., Riley, W. J., Schaefer, K., Schuur, E. A. G., Jorgenson, M. T., and Hinzman, L. D.: Empirical estimates to reduce modeling uncertainties of soil organic carbon in permafrost regions: a review of recent progress and remaining challenges, Environ. Res. Lett., 8, 035020,doi:10.1088/1748-9326/8/3/035020, 2013.

Morgenstern, A., Grosse, G., Günther, F., Fedorova, I., and Schirrmeister, L.: Spatial analyses of thermokarst lakes and basins in Yedoma landscapes of the Lena Delta, The Cryosphere, 5, 849–867, doi:10.5194/tc-5-849-2011, 2011.

Myhre, G., Highwood, E. J., Shine, K. P., and Stordal, F.: New estimates of radiative forcing due to well mixed greenhouse gases, Geophys. Res. Lett., 25, 2715–2718, 1998.

Olefeldt, D., Turetsky, M. R., Crill, P. M., and McGuire, A. D.: Environmental and physical controls on northern terrestrial methane emissions across permafrost zones, Glob. Change Biol., 19, 589–603, doi:10.1111/gcb.12071, 2013.

Osterkamp, T. E.: Causes of warming and thawing permafrost in Alaska, Eos T. Am. Geophys. Un., 88, 522–523, doi:10.1029/2007EO480002, 2007.

Plug, L. J. and West, J. J.: Thaw lake expansion in a two-dimensional coupled model of heat transfer, thaw subsidence, and mass movement, J. Geophys. Res.-Earth, 114, F01002, doi:10.1029/2006JF000740, 2009.

Raynolds, M. K., Walker, D. A., Ambrosius, K. J., Brown, J., Everett, K. R., Kanevskiy, M., Kofinas, G. P., Romanovsky, V. E., Shur, Y., and Webber, P. J.: Cumulative geoecological effects of 62 years of infrastructure and climate change in ice-rich permafrost landscapes, Prudhoe Bay Oilfield, Alaska, Glob. Change Biol., 20, 1211–1224, doi:10.1111/gcb.12500, 2014.

BGD

11, 16599–16643, 2014

Observation-based modelling of permafrost carbon fluxes

T. Schneider von Deimling et al.

Romanovsky, V. E., Smith, S. L., and Christiansen, H. H.: Permafrost thermal state in the polar Northern Hemisphere during the international polar year 2007–2009: a synthesis, Permafrost Periglac., 21, 106–116, doi:10.1002/ppp.689, 2010.

Sannel, A. B. K. and Kuhry, P.: Warming-induced destabilization of peat plateau/thermokarst lake complexes, J. Geophys. Res.-Biogeosci., 116, G03035, doi:10.1029/2010JG001635, 2011.

Scanlon, D. and Moore, T.: Carbon dioxide production from peatland soil profiles: the influence of temperature, oxic/anoxic conditions and substrate, Soil Sci., 165, 153–160, 2000.

Schädel, C., Schuur, E. A. G., Bracho, R., Elberling, B., Knoblauch, C., Lee, H., Luo, Y., Shaver, G. R., and Turetsky, M. R.: Circumpolar assessment of permafrost C quality and its vulnerability over time using long-term incubation data, Glob. Change Biol., 20, 641–652, doi:10.1111/gcb.12417, 2014.

Schaefer, K., Lantuit, H., Romanovsky, V. E., Schuur, E. A. G., and Witt, R.: The impact of the permafrost carbon feedback on global climate, Environ. Res. Lett., 9, 085003, doi:10.1088/1748-9326/9/8/085003, 2014.

Schaphoff, S., Heyder, U., Ostberg, S., Gerten, D., Heinke, J., and Lucht, W.: Contribution of permafrost soils to the global carbon budget, Environ. Res. Lett., 8, 014026, doi:10.1088/1748-9326/8/1/014026, 2013.

Schirrmeister, L., Grosse, G., Wetterich, S., Overduin, P. P., Strauss, J., Schuur, E. A. G., and Hubberten, H.-W.: Fossil organic matter characteristics in permafrost deposits of the northeast Siberian Arctic, J. Geophys. Res., 116, G00M02, doi:10.1029/2011JG001647, 2011.

Schmidt, M. W. I., Torn, M. S., Abiven, S., Dittmar, T., Guggenberger, G., Janssens, I. A., Kleber, M., Kogel-Knabner, I., Lehmann, J., Manning, D. A. C., Nannipieri, P., Rasse, D. P., Weiner, S., and Trumbore, S. E.: Persistence of soil organic matter as an ecosystem property, Nature, 478, 49–56, 2011.

Schneider von Deimling, T., Meinshausen, M., Levermann, A., Huber, V., Frieler, K., Lawrence, D. M., and Brovkin, V.: Estimating the near-surface permafrost-carbon feedback on global warming, Biogeosciences, 9, 649–665, doi:10.5194/bg-9-649-2012, 2012.

Schuur, E. A. G., Bockheim, J., Canadell, J. G., Euskirchen, E., Field, C. B., Goryachkin, S. V., Hagemann, S., Kuhry, P., Lafleur, P. M., Lee, H., Mazhitova, G., Nelson, F. E., Rinke, A., Romanovsky, V. E., Shiklomanov, N., Tarnocai, C., Venevsky, S., Vogel, J. G., and

Zimov, S. A.: Vulnerability of permafrost carbon to climate change: implications for the global carbon cycle, Bioscience, 58, 701–714, 2008.
Schuur, E. A. G., Abbott, B. W., Bowden, W. B., Brovkin, V., Camill, P., Canadell, J. G., Chanton, J. P., Chapin III, F. S., Christensen, T. R., Ciais, P., Crosby, B. T., Czimczik, C. I., Grosse, G., Harden, J., Hayes, D. J., Hugelius, G., Jastrow, J. D., Jones, J. B., Kleinen, T., Koven, C. D., Krinner, G., Kuhry, P., Lawrence, D. M., McGuire, A. D., Natali, S. M., O'Donnell, J. A., Ping, C. L., Riley, W. J., Rinke, A., Romanovsky, V. E., Sannel, A. B. K., Schädel, C., Schaefer, K., Sky, J., Subin, Z. M., Tarnocai, C., Turetsky, M. R., Waldrop, M. P., Walter Anthony, K. M., Wickland, K. P., Wilson, C. J., and Zimov, S. A.: Expert assessment of vulnerability of permafrost carbon to climate change, Climatic Change, 119, 359–374, doi:10.1007/s10584-013-0730-7, 2013.
Segers, R.: Methane production and methane consumption: a review of processes underlying wetland methane fluxes, Biogeochemistry, 41, 23–51, 1998.
Shakhova, N., Semiletov, I., Salyuk, A., Yusupov, V., Kosmach, D., and Gustafsson, O.: Extensive methane venting to the atmosphere from sediments of the East Siberian Arctic Shelf, Science, 327, 1246–1250, 2010.
Shindell, D. T., Faluvegi, G., Koch, D. M., Schmidt, G. A., Unger, N., and Bauer, S. E.: Improved attribution of climate forcing to emissions, Science, 326, 716–718, doi:10.1126/science.1174760, 2009.
Sitch, S., Smith, B., Prentice, I. C., Arneth, A., Bondeau, A., Cramer, W., Kaplan, J. O., Levis, S., Lucht, W., Sykes, M. T., Thonicke, K., and Venevsky, S.: Evaluation of ecosystem dynamics, plant geography and terrestrial carbon cycling in the LPJ dynamic global vegetation model, Glob. Change Biol., 9, 161–185, 2003.
Slater, A. G. and Lawrence, D. M.: Diagnosing present and future permafrost from climate models, J. Climate, 26, 5608–5623, doi:10.1175/JCLI-D-12-00341.1, 2013.
Smith, L. C., Sheng, Y., MacDonald, G. M., and Hinzman, L. D.: Disappearing arctic lakes, Science, 308, 1429–1429, 2005.
Stieglitz, M., Déry, S. J., Romanovsky, V. E., and Osterkamp, T. E.: The role of snow cover in the warming of arctic permafrost, Geophys. Res. Lett., 30, 1721, doi:10.1029/2003GL017337, 2003.
Strauss, J., Schirrmeister, L., Wetterich, S., Borchers, A., and Davydov, S. P.: Grain-size properties and organic-carbon stock of Yedoma Ice Complex permafrost from

BGD
11, 16599–16643, 2014

Observation-based modelling of permafrost carbon fluxes

T. Schneider von Deimling et al.

the Kolyma lowland, northeastern Siberia, Global Biogeochem. Cy., 26, GB3003, doi:10.1029/2011GB004104, 2012.
Strauss, J., Schirrmeister, L., Grosse, G., Wetterich, S., Ulrich, M., Herzschuh, U., and Hubberten, H.-W.: The deep permafrost carbon pool of the Yedoma region in Siberia and Alaska, Geophys. Res. Lett., 40, 6165–6170, doi:10.1002/2013GL058088, 2013.
Strauss, J., Schirrmeister, L., Mangelsdorf, K., Eichhorn, L., Wetterich, S., and Herzschuh, U.: Organic matter quality of deep permafrost carbon – a study from Arctic Siberia, Biogeosciences Discuss., 11, 15945–15989, doi:10.5194/bgd-11-15945-2014, 2014.
Taylor, K. E., Stouffer, R. J., and Meehl, G. A.: An overview of CMIP5 and the experiment design, B. Am. Meteorol. Soc., 93, 485–498, doi:10.1175/BAMS-D-11-00094.1, 2011.
Turetsky, M. R., Kane, E. S., Harden, J. W., Ottmar, R. D., Manies, K. L., Hoy, E., and Kasischke, E. S.: Recent acceleration of biomass burning and carbon losses in Alaskan forests and peatlands, Nat. Geosci., 4, 27–31, 2011.
van Huissteden, J. and Dolman, A.: Soil carbon in the Arctic and the permafrost carbon feedback, Current Opinion in Environmental Sustainability, 4, 545–551, 2012.
van Huissteden, J., Berrittella, C., Parmentier, F. J. W., Mi, Y., Maximov, T. C., and Dolman, A. J.: Methane emissions from permafrost thaw lakes limited by lake drainage, Nature Climate Change, 1, 119–123, 2011.
Velichko, A. A., Catto, N., Drenova, A. N., Klimanov, V. A., Kremenetski, K. V., and Nechaev, V. P.: Climate changes in East Europe and Siberia at the Late glacial–holocene transition, Quatern. Int., 91, 75–99, doi:10.1016/S1040-6182(01)00104-5, 2002.
Walter Anthony, K. M., Anthony, P., Grosse, G., and Chanton, J.: Geologic methane seeps along boundaries of Arctic permafrost thaw and melting glaciers, Nat. Geosci., 5, 419–426, 2012.
Walter Anthony, K. M., Zimov, S. A., Grosse, G., Jones, M. C., Anthony, P. M., Iii, F. S. C., Finlay, J. C., Mack, M. C., Davydov, S., Frenzel, P., and Frolking, S.: A shift of thermokarst lakes from carbon sources to sinks during the Holocene epoch, Nature, 511, 452–456, doi:10.1038/nature13560, 2014.
Walter, B. P. and Heimann, M.: A process-based, climate-sensitive model to derive methane emissions from natural wetlands: application to five wetland sites, sensitivity to model parameters, and climate, Global Biogeochem. Cy., 14, 745–765, 2000.
Walter, K. M., Edwards, M. E., Grosse, G., Zimov, S. A., and Chapin, F. S.: Thermokarst lakes as a source of atmospheric CH_4 during the last deglaciation, Science, 318, 633–636, 2007a.

Walter, K. M., Smith, L. C., and Chapin, F. S.: Methane bubbling from northern lakes: present and future contributions to the global methane budget, Philos. T. R. Soc. A, 365, 1657–1676, 2007b.

Yi, S., Wischnewski, K., Langer, M., Muster, S., and Boike, J.: Freeze/thaw processes in complex permafrost landscapes of northern Siberia simulated using the TEM ecosystem model: impact of thermokarst ponds and lakes, Geosci. Model Dev., 7, 1671–1689, doi:10.5194/gmd-7-1671-2014, 2014.

Yoshikawa, K. and Hinzman, L. D.: Shrinking thermokarst ponds and groundwater dynamics in discontinuous permafrost near council, Alaska, Permafrost Periglac., 14, 151–160, doi:10.1002/ppp.451, 2003.

Zimov, S. A., Davydov, S. P., Zimova, G. M., Davydova, A. I., Schuur, E. A. G., Dutta, K., and Chapin, F. S.: Permafrost carbon: stock and decomposability of a globally significant carbon pool, Geophys. Res. Lett., 33, L20502, doi:10.1029/2006GL027484, 2006.

Zhang, T., Frauenfeld, O. W., and Barry, R. G.: Time series of active layer thickness in the Russian Arctic, 1930–1990, Digital media, National Snow and Ice Data Center, Boulder, CO, available at: http://data.eol.ucar.edu/codiac/dss/id=106.ARCSS160, 2006.

Table 1. Permafrost model parameters and uncertainties. Some parameters are soil pool specific (MS: mineral soils, ORG: organic soils, Y: Yedoma, RTK: refrozen thermokarst deposits (separated into surface and taberal sediments), some parameters depend on hydrologic conditions (AER: aerobic, WET: wetland anaerobic, TKL: thermokarst lake anaerobic), and some parameters depend on organic matter quality (FAST and SLOW).

Parameter	Unit	Default setting	Uncertainty range	References
Carbon inventory				
Mineral soils (MS) 0–3 m (orthels and turbels)	Pg-C	540	±40 %	Hugelius et al. (2014)
Organic soils (ORG) 0–3 m (histels)	Pg-C	120	±40 %	Hugelius et al. (2014)
Yedoma (Y) 0–15 m	Pg-C	83	±75 %	Strauss et al. (2013)
Refrozen thermokarst deposits				
$RTK_{Surface}$ (0–5 m)	Pg-C	128	±75 %	Strauss et al. (2013)
$RTK_{Taberal}$ (5–15 m)	Pg-C	114	±75 %	Walter-Anthony et al. (2014)
Fraction Fast Pool [a]	%	2.5	1–4	Dutta et al. (2006), Burke et al. (2012), Schädel et al. (2014)
Fraction Slow Pool	%	45	30–60	Sitch et al. (2003), Koven et al. (2011), Burke et al. (2012)
Carbon release				
Turnover time of aerobic slow pool at 5 °C [b]	years	25	10–40	Sitch et al. (2003), Burke et al. (2012), Dutta et al. (2006)
Ratio of production $CH_4 : CO_2^{aerobic}$		1 : 50	±50 %	Lee et al. (2012), Schuur et al. (2008), Segers (1998)
Ratio of production $CH_4 : CO_2^{anaerobic\ c}$		FAST 1 : 1	±20 %	Walter-Anthony et al. (2014)
		SLOW 1 : 7	±50 %	Lee et al. (2012)
Q_{10} sensitivity aerobic		2.5	1.5–3.5	Schädel et al. (2013) and references therein
Q_{10} sensitivity anaerobic		3.0	2–6	Walter and Heimann (2000)
CH_4 oxidation rate	%	TKL 15	10–20	see Burke et al. (2012)
		WET 40	20–60	and references therein

Discussion Paper | Discussion Paper | Discussion Paper | Discussion Paper |

BGD

11, 16599–16643, 2014

Observation-based modelling of permafrost carbon fluxes

T. Schneider von Deimling et al.

Table 1. Continued.

Parameter	Unit	Default setting		Uncertainty range	References
Permafrost thaw					
Thaw rate (MS, AER) for warm and cold permafrost[d]	$cm\,yr^{-1}\,K^{-1}$	1.0 0.1		±50 % ±50 %	Frauenfeld et al. (2004), Hayes et al. (2014), Schaphoff et al. (2013)
Scale factor thermal diffusivity WET : AER[e]		1/3		±30 %	see [e]
Scale factor thermal diffusivity TKL : AER[e]		9.3		±30 %	Kessler et al. (2012)
Wetland description					
Wetland extent [f] (pre-industrial)	%	MS	2	±50 %	GLWD,
		ORG	60	±10 %	Lehner and Döll (2004),
		Y, RTK	40	±10 %	Burke et al. (2012)
Maximum increase in wetland extent[g] (above pre-industrial)		MS	30	±50 %	Gao et al. (2013)
	%	ORG, Y, RTK	10	±50 %	
Thermokarst description					
Newly formed thermokarst lake fraction F^{TKLmax}	%	MS	8	±25 %	see the Supplement
	(coverage	ORG	16	±25 %	
	per latitude)	Y	40	±25 %	
		RTK	25	±25 %	
High latitude temperature anomaly dT'^{TKLmax} at F^{TKLmax} [h]	°C		5	4–6	see the Supplement

[a] For Yedoma deposits, we assume a doubled labile fraction (5 ± 3 %) as sedimentation of organic material was rather fast and had favoured the burial of fresh organic carbon with little decomposition in the past (Strauss et al., 2012). In contrast, we assume a reduced labile fraction in taberal sediments of 1 % as these deposits had been thawed over long timescales in the past and are therefore depleted in high quality organic matter (Walter et al., 2007b; Kessler et al., 2012).

[b] We assume the turnover time of the fast pool to be one year.

[c] We discard very small ratios of $CH_4 : CO_2^{anaerobic}$ inferred from incubation experiments as it is likely that these ratios are strongly affected by a large CO_2 pulse during the initial phase of the incubation.

[d] Indicated thaw rates are exemplary for warm and cold permafrost (corresponding to a MAGT of just below 0 and −10 °C). They were calculated based on Eq. (1) (Supplement) by assuming that above-zero temperatures prevail during four months per year and that thaw is driven by a surface temperature warming anomaly of 1 °C.

[e] We prescribe aggregated thermal diffusivities for soils under aerobic conditions and use scale factors to determine modified thermal diffusivities under anaerobic conditions. Based on observational evidence (Romanovsky et al., 2010), we assume reduced thaw rates for the wetland pools as water-saturated soils require an increased latent heat input for thaw of ice-filled pore volumes. For the thermokarst soil carbon pools, we tuned scaling factors to reproduce long-term behaviour of talik propagation as simulated by Kessler et al. (2012).

[f] Based on the GLWD database, Burke et al. (2012) estimate an area coverage of 9 % for wetlands and 3 % for lakes for all permafrost regions. Based on calculated permafrost deposit extents (Hugelius et al., 2014), we estimate an area weighting of 80 : 15 : 2.5 : 2.5 % for the permafrost extents of our four soil pools (MS : ORG : Y : RTK). This results in a total weighted initial wetland extent of about 13 %.

[g] The potential for increases in wetland extent in mineral soils is considered larger than for the other soil pools because the initial assumed wetland fraction in mineral soils is rather small.

[h] Early Holocene warming by a few degrees Celsius in Northern Hemisphere land areas (Kaufman et al., 2004; Velichko et al., 2002; Marcott et al., 2013) resulted in rapid and intensive thermokarst activity (Walter et al., 2007a; Brosius et al., 2012).

Table 2. Cumulated carbon fluxes and increase in global average surface temperature through newly thawed permafrost in the years 2050, 2100, 2200 and 2300. Median and 68 % ranges (in brackets) were calculated from an ensemble of 500 model runs which account for parameter uncertainty.

	2050	2100	2200	2300
RCP2.6				
cumulated CO_2 [Pg-C]	17 (8 29)	36 (20 58)	56 (35 89)	64 (40 98)
cumulated CH_4 [Tg-CH_4]	173 (85 354)	446 (218 921)	818 (410 1753)	1035 (539 2236)
dT (PF) [°C]	0.03 (0.01 0.05)	0.06 (0.03 0.10)	0.10 (0.06 0.15)	0.11 (0.06 0.18)
RCP4.5				
cumulated CO_2 [Pg-C]	18 (9 32)	54 (28 92)	118 (75 180)	155 (104 216)
cumulated CH_4 [Tg-CH_4]	227 (109 466)	1126 (538 2356)	3117 (1657 5969)	4705 (2592 8449)
dT (PF) [°C]	0.03 (0.01 0.05)	0.08 (0.05 0.14)	0.16 (0.10 0.25)	0.19 (0.13 0.29)
RCP6.0				
cumulated CO_2 Pg-C]	18 (8 30)	60 (29 101)	156 (103 224)	193 (134 270)
cumulated CH_4 [Tg-CH_4]	201 (97 407)	1270 (663 2440)	3104 (1818 5372)	4615 (2664 7778)
dT (PF) [°C]	0.03 (0.01 0.05)	0.08 (0.04 0.13)	0.18 (0.11 0.29)	0.24 (0.16 0.39)
RCP8.5				
cumulated CO_2 [Pg-C]	20 (9 36)	87 (42 141)	194 (136 270)	228 (157 313)
cumulated CH_4 [Tg-CH_4]	333 (154 665)	1474 (836 2614)	3592 (2141 6093)	5877 (3644 9989)
dT (PF) [°C]	0.03 (0.02 0.05)	0.09 (0.05 0.14)	0.14 (0.10 0.21)	0.16 (0.11 0.23)

BGD
11, 16599–16643, 2014

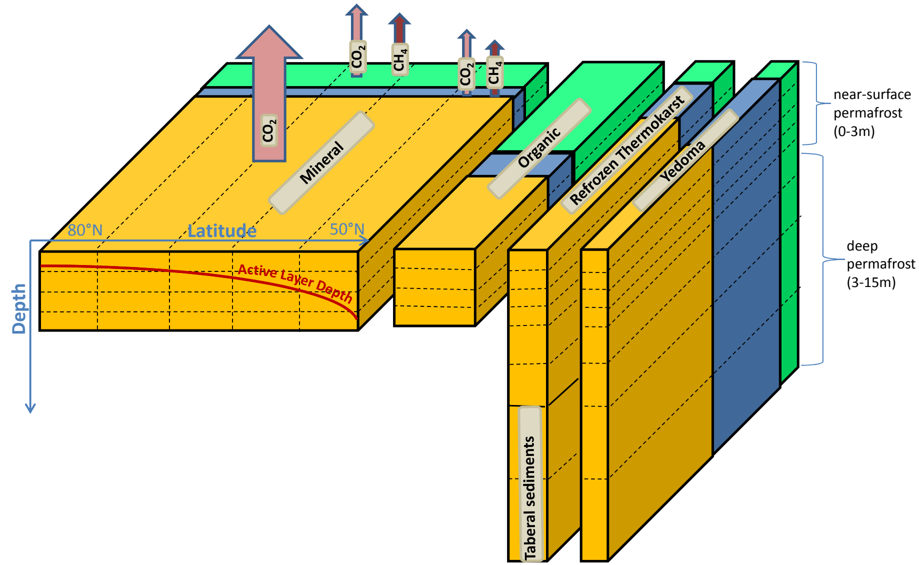

Figure 1. Schematic subdivision of permafrost soil carbon stocks into the four main pools (mineral soils, organic soils, refrozen thermokarst deposits (including taberal), and Yedoma deposits) and into aerobic (dark yellow) and anaerobic (blue: thermokarst lake, green: wetland) fractions. Individual boxes indicate the vertical extent and overall soil carbon quantity, as well as the aerobic and anaerobic fractions (not fully to scale). The dashed lines illustrate the model resolution into latitudinal bands (only shown for the mineral soil carbon pool) and vertical layers. Exemplarily, for the mineral soil carbon pool the North–South gradient of active layer depth (red line) and soil carbon release as CO_2 and CH_4 are also shown (broad arrows). Not shown is the additional differentiation into a fast and slow pool component.

BGD
11, 16599–16643, 2014

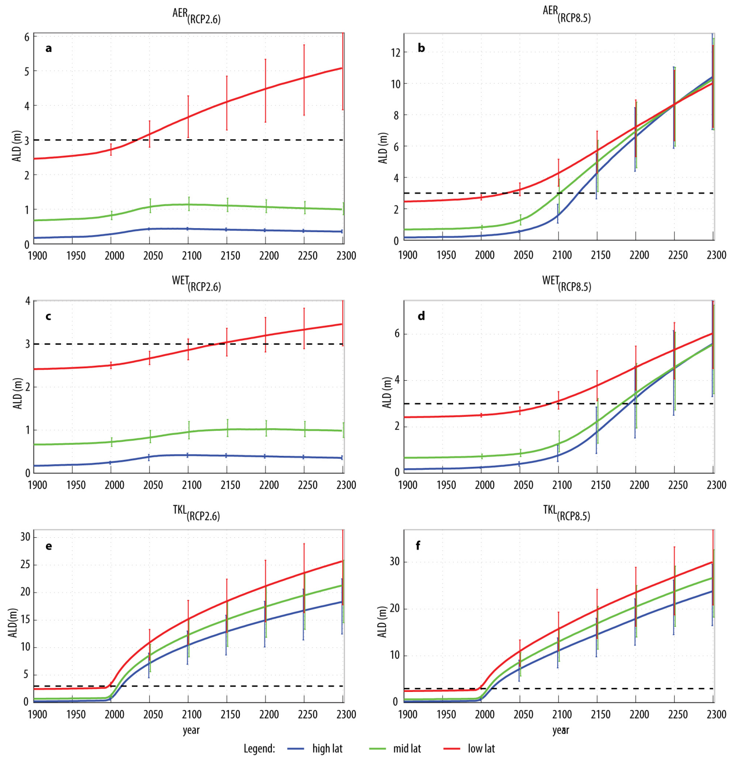

Figure 2. Simulated changes in active layer depths ALD for mineral soils under moderate (RCP2.6) and extensive (RCP8.5) warming (left and right panels). Shown is the deepening of the active layer from the year 1900 until 2300 for a north–south gradient of different initial permafrost temperatures (blue: MAGTt0 = −10 °C, green: MAGTt0 = −5 °C, red: MAGTt0 = −0.5 °C) and for different hydrologic conditions (**a, b**: aerobic, **c, d**: wetland, **e, f**: thermokarst lake). Vertical bars illustrate the model spread inferred from an ensemble of 500 runs (68 % range). The horizontal dashed lines denote the near-surface permafrost boundary (3 m). Note the different *y* axes scales.

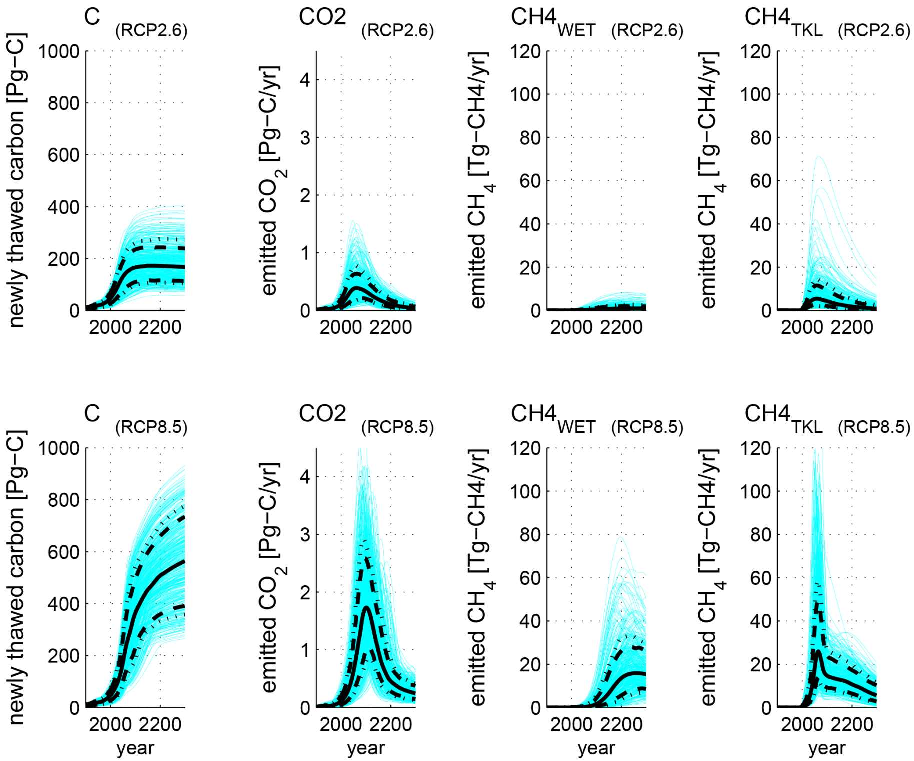

Figure 3. Simulated increase in newly thawed permafrost carbon C and resulting rates of annual CO_2 and CH_4 release under moderate (upper panels) and extensive (lower panels) global warming for the years 1900 to 2300. CH_4 release is shown separately for fluxes from wetland (WET) and thermokarst lake (TKL) pools. Blue lines show ensemble simulation results based on 500 model runs which account for parameter uncertainty. Black lines show statistical quantiles (solid line: median, dashed lines: 68 % range, dotted lines: 80 % range). Shown are contributions aggregated over all individual pools, summed over all latitudes and depths layers.

BGD
11, 16599–16643, 2014

Observation-based modelling of permafrost carbon fluxes

T. Schneider von Deimling et al.

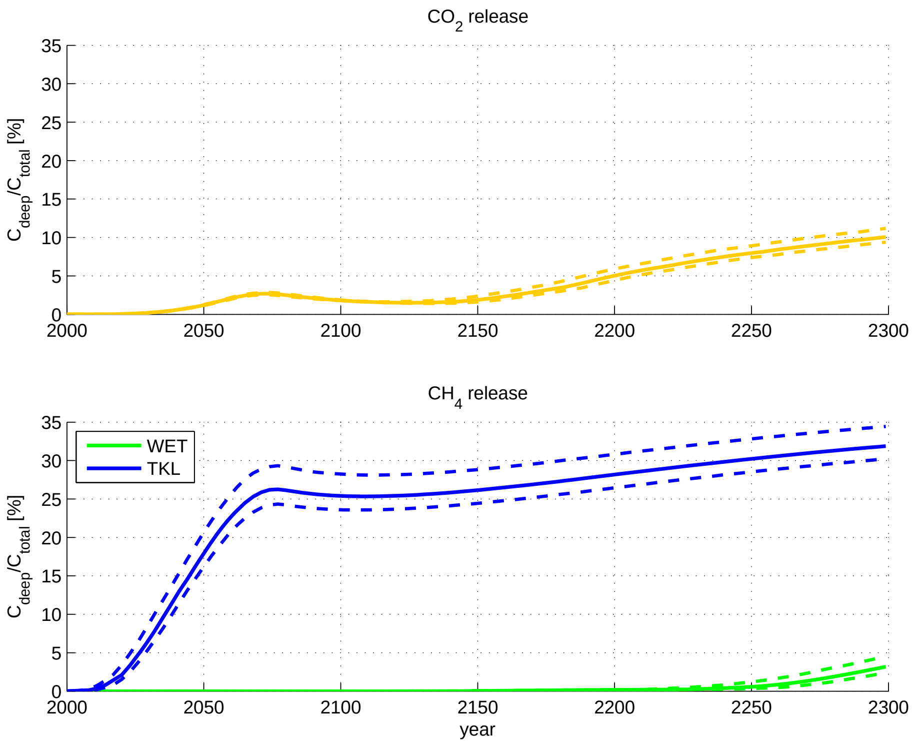

Figure 4. Contribution of deep permafrost carbon deposits to total carbon fluxes under aerobic (upper panel) and anaerobic (lower panel) conditions. Shown is the contribution of cumulated CO_2 and CH_4 fluxes from deep deposits (3–15 m) to total circumarctic carbon release (0–15 m) under strong warming (RCP8.5). Solid lines represent median values, dashed lines 68 % ranges. CH_4 release is shown separately for wetland-affected sediments (green) and for thermokarst-affected sediments (blue).

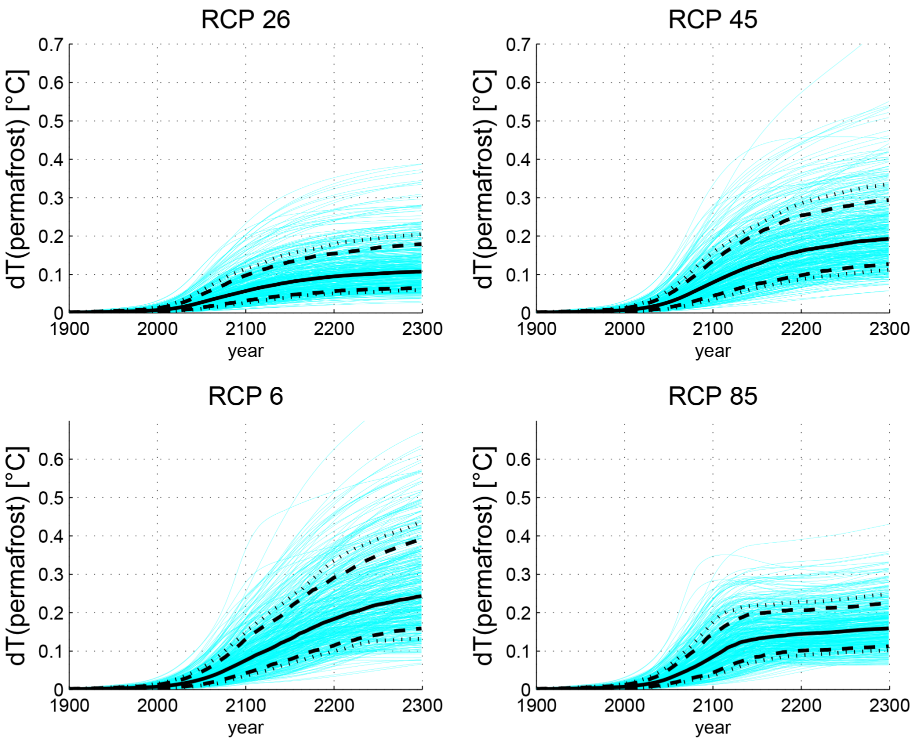

Figure 5. Increase in global average surface air temperature through newly thawed permafrost carbon under various anthropogenic warming scenarios (RCP2.6 to RCP8.5). Blue lines show ensemble simulation results based on 500 model runs which account for parameter uncertainty. Black lines show statistical quantiles (solid line: median, dashed lines: 68 % range, dotted lines: 80 % range). Shown is the temperature feedback as a consequence of CO_2 and CH_4 release from all individual pools.

BGD
11, 16599–16643, 2014